

# 1024-Channel-Scalable Wireless Neuromonitoring and Neurostimulation Rodent Headset with Nanotextured Flexible Microelectrodes

A. Bagheri\*, S. R. I. Gabran†, M. T. Salam\*, J. L. Perez Velazquez‡, R. R. Mansour†, M. M. A. Salama†, R. Genov\*

\*Department of Electrical and Computer Engineering, University of Toronto, Canada, Email: arezu@eecg.utoronto.ca

†Department of Electrical and Computer Engineering, University of Waterloo, Canada

‡Brain and Behaviour Centre, Division of Neurology, University of Toronto, Canada

**Abstract**—We present a compact wireless headset system for simultaneous multi-site neural recording and neurostimulation in the rodent brain. The system comprises flexible-shaft microelectrodes, neural amplifiers, neurostimulators, a digital time-division multiplexer (TDM), a micro-controller and a ZigBee wireless transceiver. The system is built by parallelizing up to four 0.35 $\mu\text{m}$  CMOS integrated circuits (each having 256 neural amplifiers and 64 neurostimulators) to provide a total maximum of 1024 neural amplifiers and 256 neurostimulators. Each bipolar neural amplifier features 54dB-72dB adjustable gain, 1Hz-5KHz adjustable bandwidth with an input-referred RMS noise of 7.99 $\mu\text{V}$  and dissipates 12.9 $\mu\text{W}$ . Each current-mode bipolar neurostimulator generates arbitrary waveform programmable biphasic currents in the range of 20-250 $\mu\text{A}$  and dissipates 2.6 $\mu\text{W}$  in the stand-by mode. Reconfigurability is enabled by stacking a set of dedicated mini-PCBs that share a common signaling bus within as small as 22 $\times$ 30 $\times$ 15mm<sup>3</sup> volume. The system features flexible polyimide-based microelectrode array design that maximizes pad packing density. Electrodeposition pad nanotexturing reduces the electrode-tissue interface impedance from an average of 2M $\Omega$  to 30K $\Omega$  at 100Hz. The system has been validated *in vivo* in Sprague-Dawley rats.

## I. INTRODUCTION

Simultaneous monitoring of electrical neural activity at many locations in the brain provides electrographic data with high spatial resolution. This enables investigation of the behavior of a large population of neurons and comprehensive neural activity assessment required for developing state-of-the-art neural prostheses, such as for treatment of medically refractory epilepsy [1]. Simultaneous electrical current stimulation localized at many sites in the brain allows for fine-tuned neurostimulation therapies optimized to a given neural disorder and custom tailored to each specific patient, potentially increasing their efficacy. Combining both neural monitoring and neural stimulation in a single implantable device enables responsive neural stimulation, where stimulation is triggered by detected neural events, a promising paradigm in modern neuro-rehabilitation.

A steady increase in the number of monitored sites in the brain has been observed, approximately doubling every seven years [2]. Expanding the number of recording and stimulation sites introduces several challenges including noise, power consumption and form factor of electronic neural interfacing

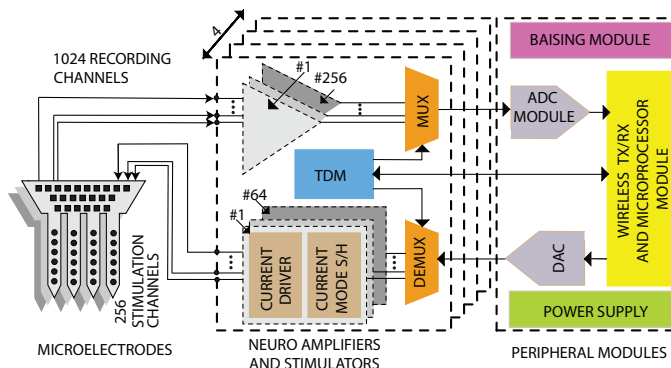


Fig. 1. System-level block diagram.

circuits as well as impedance and fragility of microelectrodes.

Multi-channel commercial neural recording and stimulation systems for humans do not interface with many recording or stimulation sites (e.g., currently up to eight for responsive neurostimulation for treatment of medically refractory epilepsy). Animal models of neurological disorders, particularly rodent models, are widely accepted as low-cost vehicles for developing state-of-the-art neural prostheses. Commercial neural recording and stimulation products for implantation in rodents currently offer up to 32 channels [3]. In academia, Neurochip-2 at University of Washington has been very successful but weighs 145g and has only three recording and stimulation channels [4]. HermesD at Stanford University has 32 recording channels but no neurostimulation channels [5]. A number of other state-of-the-art headset designs have been reported [6], [7], but either have a limited number of channels, or lack neurostimulation, or have a large form factor.

Several microelectrode designs, mostly silicon-based, have been developed for multi-site neural recording and stimulation [8], [9]. Silicon electrodes can cause post-operative trauma and damage to brain tissue due to their rigid nature. Silicon structures are brittle, and prone to mechanical failure and to releasing debris in the brain. Additionally, the high packing density requirement necessitates smaller size of each tissue contact, increasing its impedance, thus degrading the recording signal-to-noise ratio and the maximum stimulation current for

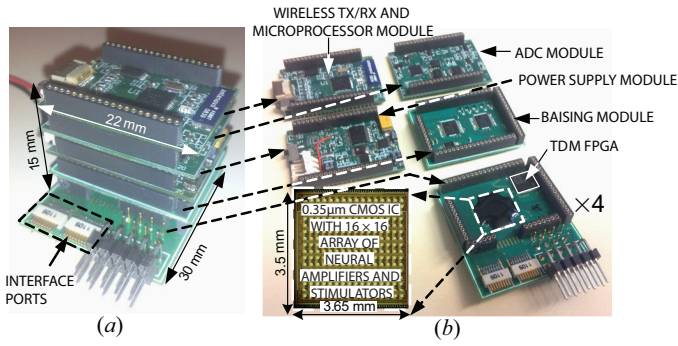


Fig. 2. Wireless headset: (a) assembled stack and (b) individual boards.

a given supply voltage.

In this paper, we present a compact wireless rodent headset with a maximum channel count of 1024 for simultaneous neural recording, and 256 for simultaneous neural stimulation. It is interfaced with flexible-shaft microelectrode arrays with tissue contact surface modified by nanotexturing to reduce its impedance on average by a factor of over 60. The system targets simultaneous large-scale neural monitoring, spatially-rich neural stimulation and closed loop neurostimulation for monitoring and treatment of medically refractory epilepsy.

## II. METHODS AND MATERIALS

The head-mounted system is comprised of two components: an electronic headset and a flexible microelectrode array.

### A. Rodent Headset

The headset system consists of 2 core and 3 optional stacked miniature printed circuit boards (PCBs) as shown in Fig. 2. Each module provides circuits for a distinct function, as described next.

1) *Neural Amplifiers and Stimulators (Core) Module:* A neuro-interface integrated circuit was designed to provide 256 recording and 64 stimulation channels [10]. The chip is wire-bonded onto a 22mm×30mm PCB module and protected by epoxy. Four of these modules can be stacked to provide 1024 simultaneous recording channels and 256 stimulation channels. In this prototype only 64 channels were used for experimental testing.

The amplifier in each channel has a programmable mid-band gain from 54dB to 72dB, programmable bandwidth of 1Hz to 5KHz with  $7.99\mu V_{rms}$  input-referred noise, and consumes  $12.9\mu W$  [10]. Microelectrodes are connected to the amplifier in a bipolar fashion through four Omnetics connector ports. A low-power FPGA performs time-domain multiplexing of these channels.

The bipolar stimulators feature charge-balanced symmetric biphasic stimulation which provides control over the charge delivered to the tissue. The charge density is limited to  $60\mu C/cm^2$  per phase to prevent tissue damage [11]. The stimulation current ranges from 20 to  $250\mu A$  and each stimulator consumes  $2.6\mu W$  quiescent power. Each stimulation channel can be individually addressed and the stimulation

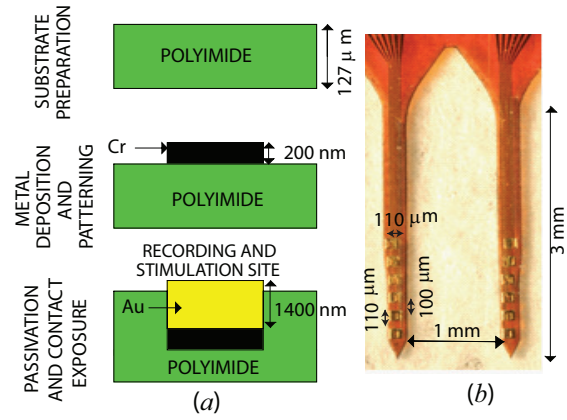


Fig. 3. 2-D microelectrode array: (a) fabrication process and (b) dimensions.

parameters are set by the on-board FPGA. A group of selected stimulation channels provide simultaneous stimulation without multiplexing.

2) *Biasing (Core) Module:* The bias voltages and currents required by the neural recording and stimulation chip are generated by a set of DACs.

3) *Power Supply (Optional) Module:* The power supply module provides multiple regulated source voltages for different circuits of the system.

4) *ADC (Optional) Module:* The analog recorded data, is fed to the ADC module to digitize the data.

5) *Wireless Tx/Rx and Microprocessor (Optional) Module:* The digital data packets received from the ADC module can be transmitted through a ZigBee wireless connection. Commands can be wirelessly received through the same interface. A TI microcontroller can be used in a closed-loop configuration. The wireless interface is included to facilitate debugging of the neurostimulator in the closed-loop configuration.

This system weighs 12g, is powered by a Lithium-sulfur dioxide battery (not shown) and can operate for 10 hours continuously. Mini-PCBs in items 3 to 5 were designed and fabricated by Canadian Microelectronics Corporation (CMC), in a joint research project.

### B. Flexible Microelectrode Array

The microelectrodes provide a 2-D array of neural interfacing sites capable of both neural recording and stimulation through large-area pads. The electrode architecture was developed to maximize channel packing and was employed to create an array of shafts. Each shaft has a width of  $130\mu m$  and accommodates six  $110\mu m \times 110\mu m$  pads. The array is implemented on a flexible polyimide substrate with gold metallization layers. During insertion, the electrode is subjected to axial and shear loading and is susceptible to buckling failure which inhibits tissue penetration. The electrode structure is designed to survive the mechanical forces experienced during tissue penetration and has a small footprint to reduce tissue trauma and improve biocompatibility. The design scales up to 1024 sites by increasing the number of shafts and layering

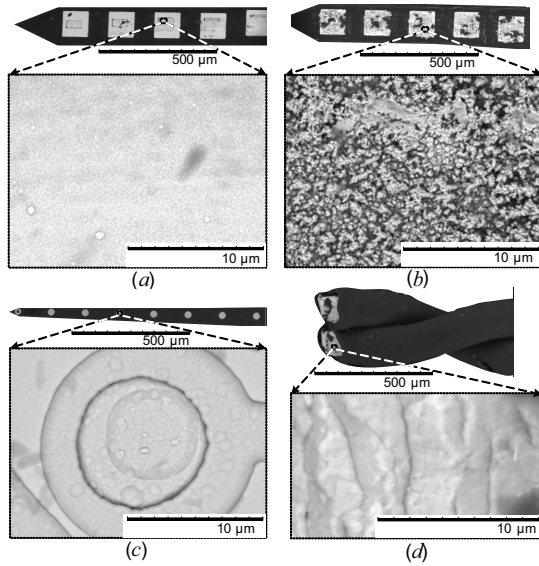


Fig. 4. Scanning electron microscope (SEM) images of: (a) smooth-surface microelectrode (SME), (b) nanotextured microelectrode (NME), (c) commercial microelectrode (CME), and (d) commercial microwire (CMW).

multiple substrates onto each other. This has been experimentally validated.

1) *Fabrication Process*: A gold thin film is formed on a polyimide substrate by DC sputtering deposition using chromium as an adhesion layer. After metal layer patterning, polyimide passivation layer is spin coated and dry etched to expose the contact pads. A second metal layer is deposited and patterned to raise the pad profile. Finally, the electrode is diced and released using laser micromachining [12].

2) *Electrode Contact Surface Modification*: The resulting smooth-surface microelectrodes (SME) have a high electrode-tissue interface impedance ( $\sim 2\text{M}\Omega$  at 100Hz). A pad surface modification technique was developed using low-current pulsed electroplating process. The resulting nanotextured electrodes (NME) exhibit rough surface and an average impedance of  $\sim 30\text{k}\Omega$  at 100Hz.

### III. EXPERIMENTAL RESULTS

The system has been used in comparing the performance of several electrodes including smooth-surface microelectrodes (SME), nanotextured microelectrodes (NME), commercial thin film microelectrodes (CME) and commercial microwire electrodes (CMW). Fig. 4 presents the scanning electron microscope (SEM) images of the electrodes. The close-up views in Fig. 4 illustrate the surface condition of the metal contacts. The NME exhibits the most roughened surface with the desired nano-scale structures clearly seen and yields the lowest impedance, as described next.

#### A. Microelectrodes Characterization

The electrode-tissue interface impedance of the presented and the commercial electrodes were measured using standard two electrode electrochemical cell with 0.9% saline solution.

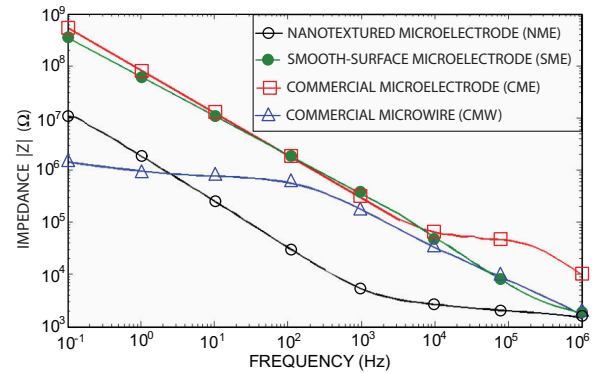


Fig. 5. Measured impedance of the presented and commercial electrodes.

The impedance Bode plots for the electrodes, obtained by impedance spectroscopy (Solatron SI 1260 Impedance/Gain-Phase Analyzer), are shown in Fig. 5. The presented rough surface nanotextured microelectrode (NME) exhibits significantly lower impedance in the 10Hz to 100kHz frequency band due to the increased effective surface area.

Electrode-electrolyte noise was measured using a large (2cm $\times$ 2cm) surface platinum reference plate in a standard physiological saline solution. Fig. 6 illustrates electrode-electrolyte noise densities of the presented and commercial electrodes. The NME has the lowest noise density due to the lower impedance.

#### B. In vivo Neural Signal Recording Performance

These studies were conducted at the Neurosciences & Mental Health Research Institute of Hospital for Sick Children (Canada) with an approval from the ethics committee. The headset system was tested chronically *in vivo* in freely moving rats. The recording performance of the four electrode types was evaluated in acute recordings using the headset system.

1) *Chronic Recordings*: Dawley rats (weight:150-250g) were injected (intraperitoneally) with kainic acid to induce a chronic epilepsy model. Three weeks after the injection, CMW electrodes were implanted in both hippocampi of the rats. Neural signals were recorded at 200Hz sampling rate using the headset system and a commercial amplifier (Biopac Inc.) in order to validate the recording system. Fig. 7 shows electrographic seizure recordings from a rat (8 weeks after the injection) using the presented and commercial systems. The long-term recordings are stable without a significant decrement in signal quality for up to 9 weeks after implantation.

2) *Acute Recordings*: One Dawley rat underwent a craniotomy with general anaesthesia. Through the craniotomy windows, four types of microelectrodes (Fig. 4) were implanted into the somatosensory area. Bipolar recordings were performed using the headset system. The recorded signals have been analyzed in several frequency bands (e.g., delta 0.1-4Hz, theta 4-7Hz, alpha 8-13Hz, beta 13-30Hz, gamma 30-100Hz). The mean field potential power in each band was measured in order to evaluate the recording quality, as shown in Fig. 8. Fig. 8 illustrates that SME and CME exhibit higher low-

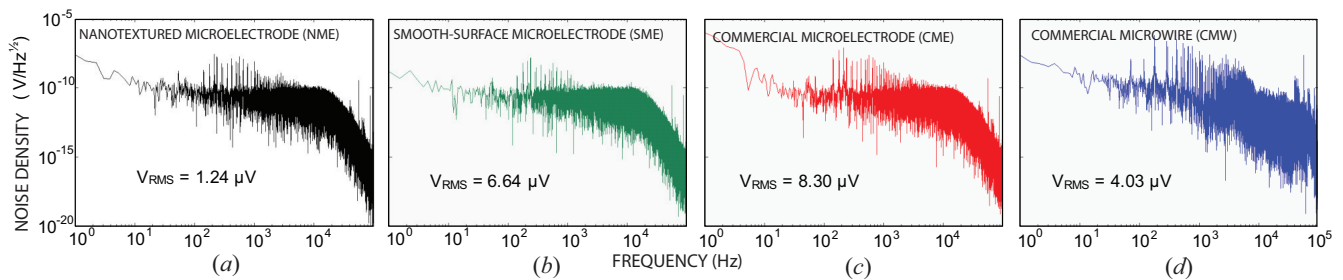


Fig. 6. Measured electrode noise spectral densities of the presented and commercial electrodes.

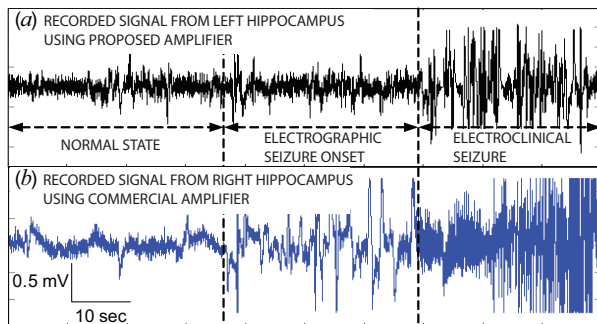


Fig. 7. Neural signal recording *in vivo* using: (a) the presented headset system and (b) a commercial amplifier.

frequency noise whereas the low-frequency noise is suppressed when using NME and CMW. Fig. 8 also demonstrates that at high frequencies, CMW exhibits higher thermal noise whereas NME yields the best signal fidelity.

#### IV. CONCLUSION

A compact wireless headset system with a flexible microelectrode array has been presented. The headset system scales up to 1024 and 256 channels for neural recording and stimulation, respectively. Electrodeposition surface modification increases the effective surface area of the electrode contacts, yielding lower input impedance and improved interfacial capacitance. This translates into over 60 times reduction in the impedance at 100Hz and four times less noise density compared to smooth-surface and commercial electrodes.

#### ACKNOWLEDGMENT

The authors thank Natural Sciences and Engineering Research Council of Canada, Ontario Brain Institute and the Canadian Microelectronics Corp. (CMC) for their financial and technical support.

#### REFERENCES

- [1] M. Fifer, S. Acharya, H. Benz, M. Mollazadeh, N. Crone, and N. Thakor, "Toward electrocorticographic control of a dexterous upper limb prosthesis: Building brain-machine interfaces," *IEEE Pulse*, vol. 3, no. 1, pp. 38–42, Jan. 2012.
- [2] I. H. Stevenson and K. P. Kording, "How advances in neural recording affect data analysis," *Nature Neuroscience*, vol. 14, pp. 139–142, Jan. 2011.
- [3] Ripple: Grapevine nano. Accessed on Jun 1, 2012, <<https://www.rppl.com/products/grapevine-front-ends/item/133-grapevine-nano>>.

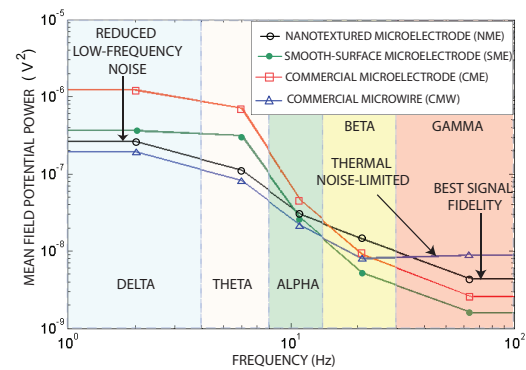


Fig. 8. Field potential power recorded from somatosensory area using the presented and commercial electrodes.

- [4] S. Zanos, A. Richardson, L. Shupe, F. Miles, and E. Fetz, "The neurochip-2: An autonomous head-fixed computer for recording and stimulating in freely behaving monkeys," *IEEE Transactions on Neural Systems and Rehabilitation Engineering*, vol. 19, no. 4, pp. 427–435, Aug 2011.
- [5] H. Miranda, V. Gilja, C. Chestek, K. Shenoy, and T. Meng, "Hermesd: A high-rate long-range wireless transmission system for simultaneous multichannel neural recording applications," *IEEE Transactions on Biomedical Circuits and Systems*, vol. 4, no. 3, pp. 181–191, June 2010.
- [6] R. Harrison, R. Kier, C. Chestek, V. Gilja, P. Nuyujukian, S. Ryu, B. Greger, F. Solzbacher, and K. Shenoy, "Wireless neural recording with single low-power integrated circuit," *IEEE Transactions on Neural Systems and Rehabilitation Engineering*, vol. 17, no. 4, pp. 322–329, Aug. 2009.
- [7] C. P. Young, S. F. Liang, D. W. Chang, Y. C. Liao, F. Z. Shaw, and C. H. Hsieh, "A portable wireless online closed-loop seizure controller in freely moving rats," *IEEE Transactions on Instrumentation and Measurement*, vol. 60, no. 2, pp. 513–521, Feb. 2011.
- [8] R. Vetter, R. Miriani, B. Casey, K. Kong, J. Hetke, and D. Kipke, "Development of a microscale implantable neural interface (mini) probe system," in *27th Annual International Conference of the Engineering in Medicine and Biology Society, IEEE-EMBS*, Jan. 2005, pp. 7341–7344.
- [9] R. H. Olsson and K. D. Wise, "A three-dimensional neural recording microsystem with implantable data compression circuitry," *IEEE Journal of Solid-State Circuits*, vol. 40, no. 12, pp. 2796–2804, Dec. 2005.
- [10] R. Shulzycki, K. Abdelhalim, A. Bagheri, C. Florez, P. Carlen, and R. Genov, "256-site active neural probe and 64-channel responsive cortical stimulator," in *IEEE Custom Integrated Circuits Conference (CICC)*, Sep. 2011.
- [11] T. L. Skarpaas and M. J. Morrell, "Intracranial stimulation therapy for epilepsy," *Neurotherapeutics*, vol. 6(2), pp. 238–43, Apr. 2009.
- [12] S. Gabran, R. Mansour, and M. Salama, "Maskless pattern transfer using 355nm laser," *Optics and Lasers in Engineering*, vol. 50, no. 5, pp. 710–716, 2012.